Insight into Structure-Dependent Self-Activation Mechanism in a Confined Nanospace of Core–Shell Nanocomposites

*Qiang Sun, Wen-Cui Li, and An-Hui Lu**

Rational design and manipulation of core-shell composites with nanometer-scale precision of building blocks can be achieved nowadays.[1–3] Core-shell nanostructures with diverse core structures and shell compositions present a class of novel materials which bring new opportunities for active encapsulation,[4,5] high efficiency catalysis,[6–9] superior energy storage,[10,11] and targeted drug delivery.[12,13] Silica-based core-shell composites have been the most widely studied so far, particularly in nanoreactor design owing to the versatile silica chemistry.[14–20] For example, it has been shown that the outer silica shell creating a confined environment is permeable and the active component cores can be accessed by solvents and reactants.[17–20] To date, little attention has yet been paid to the influence of the shell's porosity on the structure development of the whole composite, though core-shell composites are excellent model systems for size-matter effect studies. In particular, when the composite is subject to a high temperature annealing, conceivably, the structure evolution in the core-shell composites can be very different due to the different physical and chemical properties of the core and the shell. Experimental studies in this field are still scarce, and molecular interactions at the interface in a confined environment are not clear, despite impressive advances and sophisticated knowledge in synthesis and assembly of core-shell composites on the level of molecular constructs during last two decades.

To address this issue, we herein report a new finding of the structure-dependent self-activation mechanism in a confined nanospace of core-shell nanocomposites. That was when a hollow polymer nanosphere was encapsulated with silica and then subjected to pyrolysis, the core was observed to enlarge by self-activation mechanism and the phenomenon was sensitive to the pore open or close state of the outer silica shell (**Figure 1**). To our knowledge, this phenomenon which is associated with the confined effect has never been reported in the large body of publications on core-shell composites. The core expansion mechanism is different from previous reports where the expansion of the hollow core was realized by adjusting the hard-template size.[21]

Firstly, hollow polymer nanospheres (HPS) were synthesized according to a previous study (see the Supporting Information for details). The synthesis principle was based on the weak acid-base interaction ($-COO^-/NH4^+/-COO^-$) induced assembly, using 2, 4-dihydroxybenzoic acid and formaldehyde as the precursors, oleic acid as the soft template, and ammonia as the base catalyst.[22] The diameter of the HPS is *ca.* 200 ± 15 nm and the hollow core is *ca.* 40 ± 5 nm. Hollow carbon spheres with a hollow core diameter of *ca.* 55 ± 5 nm, denoted as HCS-1, can be obtained by carbonization of HPS. In order to create a confined environment on the external surface of each HPS, HPS were coated with a silica shell via a modified Stöber process, using the surfactant cetyltrimethyl-ammonium bromide (CTAB) as the structure directing agent.[23] As a consequence, a core-shell composite, denoted as HPS@SiO_2 was obtained. The driving force for the silica shell formation was the electrostatic interaction between the anionic polymer surface (Figure S1) and the cationic CTAB micelles.[24] In Figure 1 and Figure S2a, the TEM images of HPS@SiO_2 show that the silica shell thickness is *ca.* 45 ± 5 nm. Pyrolysis of HPS@SiO_2 at 800 °C under nitrogen atmosphere led to the formation of silica encapsulated hollow carbon sphere, denoted as HCS-2@SiO_2. Interestingly, the diameter of the hollow core was enlarged from 40 to 160 nm (Figure 1, and Figure S2b), whereas the outer silica shell showed a shrinkage of only *ca.* 10% before and after pyrolysis. This unusual core enlargement phenomenon was achieved by self-activation from confined effect in situ. Generally, the mesopores of the as-synthesized silica shell are closed due to the presence of the surfactant CTAB.[18,25,26] To open the mesopores of the as-synthesized composite HPS@SiO_2, one method is to reflux the composite in ethanol in the presence of an acid to remove the CTAB template.[26] In this work, CTAB-free composite was obtained by this procedure and denoted as HPS@mSiO_2 (mSiO_2 represents SiO_2 with opened mesopores). Pyrolysis of the obtained HPS@mSiO_2 under the same conditions as that of HCS-2@SiO_2 led to the formation of analogue HCS-3@mSiO_2. TEM observations showed the hollow core of HCS-3@mSiO_2 (Figure 1 and Figure S2c) was approximately 120 nm in diameter, *i.e.,* 40 nm

Q. Sun, Prof. W.-C. Li, Prof. A.-H. Lu
State Key Laboratory of Fine Chemicals
School of Chemical Engineering
Faculty of Chemical
Environmental and Biological Science and Technology
Dalian University of Technology
Dalian 116024, P. R. China
E-mail: anhuilu@dlut.edu.cn
Tel/Fax: +86-411-84986112

DOI: 10.1002/smll.201202671

small

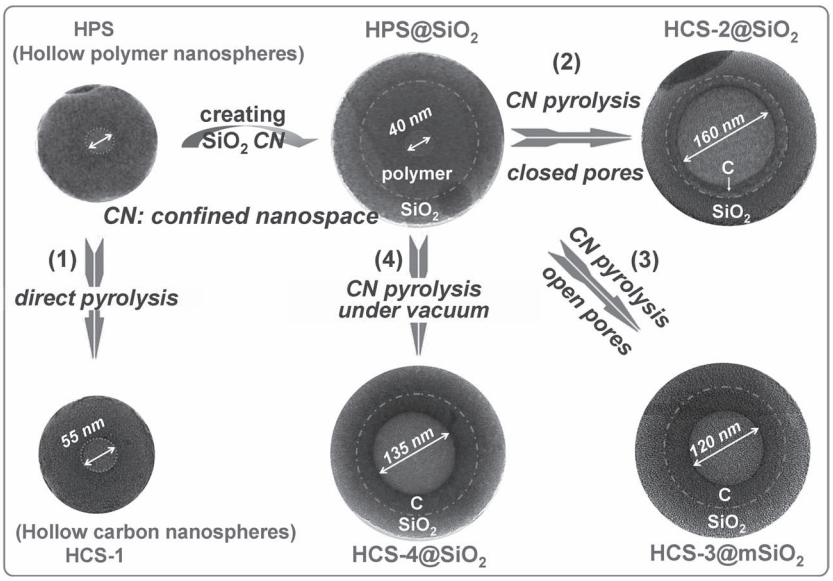

Figure 1. The formation processes of hollow carbon nanospheres.

less than that of HCS-2@SiO_2 obtained by pyrolysis when the mesopores of the confined shell were blocked. These results indicated that the confined silica shell may have played a crucial role on the core structure of HCS during the pyrolysis process.

To establish the role of the silica confinement during the confined pyrolysis, the aforementioned three samples, HPS, HPS@SiO_2, and HPS@mSiO_2, were characterized by TG-MS under N_2 with a heating rate of 10 °C min^{-1} (**Figure 2**). The exhaust gases were monitored by an online mass spectrometer (MS); combined with the thermogram, the information revealed the onset of the thermal decomposition behavior of these samples. The TG curves showed that the first stage was the removal of physically adsorbed water. In Figure 2b, the remarkable weight loss between 150~300 °C corresponded to the decomposition processes of the template species. The fragments (m/z = 58, 59) were assigned to the surfactant CTAB head group. Compared to HPS, the main peak position of CO_2 (m/z = 44), which was produced during pyrolysis of HPS@SiO_2, moved to a higher temperature of 470 °C. As known, the CO_2 released by HPS decarboxylation takes place at 300 °C,[27] and the silica shell is pressure-tight until CTAB decomposition. Supporting that the silica shell is impermeable before 300 °C, the internal pressure generated from CO_2 inside the hollow core of HPS@SiO_2 is truly immense, i.e., a whopping *ca.* 630 ~ 40000 times atmospheric pressure (see the Supporting Information for detailed estimation). Although that value is too large to imagine, as a rule of thumb, one can envisage that when the pressure within the hollow core reaches a critical value, the trapped gases would penetrate the silica and carbon shells to the outer environment. Under such high auto-generated high pressure, the confined nanospace possibly provides a "supercritical condition" that facilitates chemical reactions at lower temperature, as discussion below. Furthermore, the peak positions of CO (m/z = 28) moved to lower temperatures (Figure 2a,b). The TG-MS curves of surfactant-free sample HPS@mSiO_2 showed a clear migration of the CO_2 peak position, whereas the peak positions of the CO remained similar to that of HPS (Figure 2c). It seems that the release of CO_2 activated the polymer at low temperatures in the confined nanospace. As a result, the hollow core space increased substantially. During the pyrolysis, the amount of H_2O generated was less than that of CO_2 and CO, as evidenced by the weak intensity of the H_2O signals. By carefully examining the peak positions of the generated H_2O from HPS@SiO_2 and HPS@mSiO_2, a small peak shift was observed. Besides, fragments of H_2 are mainly detected beyond 750 °C, which are ascribed to the graphene layers aromatization.[28] The results imply that during pyrolysis, the H_2O and CO_2 generated in situ may act as the activation agents by reacting with the carbon precursor encapsulated inside the nanoreactor. One way to examine this is to calculate the eliminated volume of HCS-2@SiO_2 after confined nanospace pyrolysis according to the higher magnification TEM images in Figure 1. The calculated hollow core volumes of the three samples are listed in Table S1. The results show that after pyrolysis in the confined nanospace, the hollow core volume of HCS-2@SiO_2 was ~25 times larger than that of the HCS-1, while the volume of the carbon shell was only half of the HCS-1.

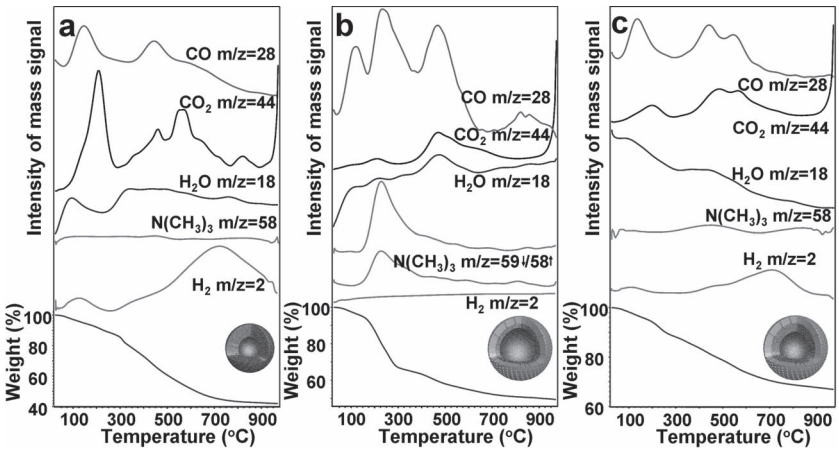

Figure 2. TG-MS measurements on the as-synthesized a) HPS, b) HPS@SiO_2, and c) HPS@mSiO_2.

As seen from Figure 2, TG-MS curves clearly demonstrated that the silica nanoreactor can retard the penetration of the in situ generated gases through the silica shell during the confined pyrolysis process. To test this, we pyrolyzed the surfactant-containing composite HPS@SiO_2 at 800 °C under continuous evacuation conditions,

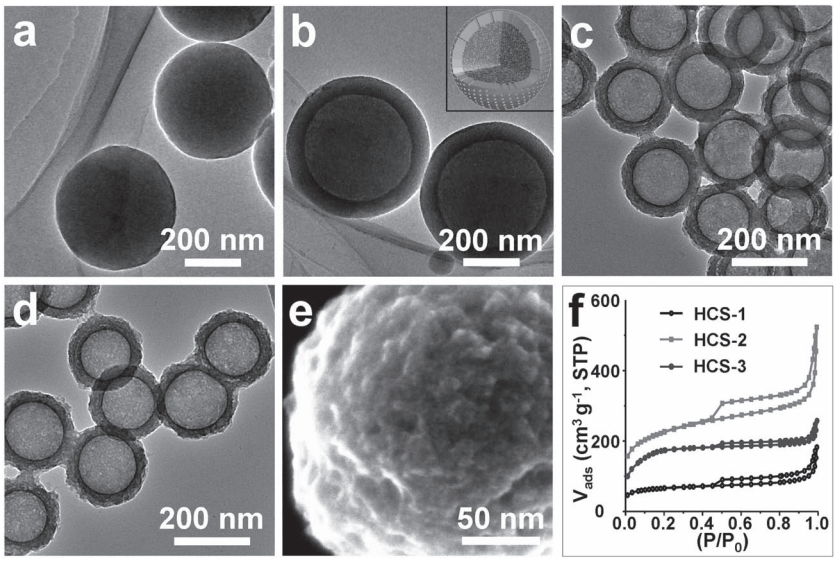

Figure 3. TEM images of a) SPS, b) SCS-2@SiO_2, c) carbon product obtained by carbonization of HPS@SiO_2 at 600 °C and subsequent silica removal process, d) HCS-2; SEM image of e) HCS-2; N_2 sorption isotherms of f) HCS-1, HCS-2 and HCS-3, the isotherm of HCS-1 is offset vertically by –60 $cm^3 g^{-1}$.

with the aim of facilitating instant removal of the gases and consequently limiting the self-activation in the confined nanospace. As seen in Figure 1 and Figure S2d, the obtained core-shell spheres (named HCS-4@SiO_2) indeed showed very similar morphology and core size as that of HCS-3@mSiO_2 pyrolyzed in the absence of surfactant. According to the TEM image in Figure 1, the hollow core volume of HCS-4@SiO_2 was ~15 times larger than that of the HCS-1. This confirmed that pyrolysis either under vacuum or with open mesopores allowed instant release of the in situ generated gases, thus avoiding carbon consumption by self-activation.

A control experiment was conducted by pyrolyzing silica coated solid polymer spheres (SPS, **Figure 3**a) to clarify the role of the hollow core. As shown in Figure 3b, the TEM image reveals that the solid carbon product (denoted as SCS-2@SiO_2) inside the confined silica nanospace retains similar morphology to the original SPS. The resultant core-shell structures remain solid with no hollow cores generated. Hence, we believe that the hollow core structure is intrinsically responsible for such an unusual core expansion during confined nanospace pyrolysis. As the TG-MS curves shown, the most pronounced gases evolution occurred under 600 °C. It would be interesting to determine if any self-activation reaction could automatically take place at such a low temperature. Thus, HPS@SiO_2 was pyrolyzed at 600 °C followed by a silica leaching procedure. As shown in Figure 3c, this indeed was the case that the hollow core diameter of the spheres increased from 40 to 160 nm. This is identical to that pyrolyzed at 800 °C. This result strongly indicates that the gasification reaction between CO_2 and H_2O and the carbon shells is facilitated even at low temperature under a perceived "supercritical condition" created by the confined nanospace during high temperature annealing. This phenomenon is considerably differing from the reactions of bulk materials which require high reaction temperature, usually exceeding 800 °C.[29,30]

After removal of the silica layer via NaOH etching, the obtained hollow carbon nanospheres (HCS-2) exhibited a perfect hollow core-shell structure (Figure 3d) with a hollow core diameter of ~160 nm and a shell thickness of ~20 nm. When HCS-2 was analyzed by SEM at a higher magnification (Figure 3e), the surface of the product was observed to be rough and irregular. The porosities of the carbon products after removal of the silica layer were analyzed by N_2 sorption at 77 K (Figure 3f). Compared with HCS-1, the specific surface area and total pore volume (estimated from the amount of adsorbed N_2 at $P/P_0 = 0.90$) of HCS-2 increased from 560 $m^2 g^{-1}$ and 0.30 $cm^3 g^{-1}$ to 787 $m^2 g^{-1}$ and 0.48 $cm^3 g^{-1}$, respectively. Owing to the high surface area of the hollow carbon nanospheres, sample HCS-2 was chosen as adsorbent for the removal of Cr(VI) from an aqueous solution. The results showed this material exhibited high efficiency for removal of Cr(VI) (see the Supporting Information and Figure S5 for details). As for the carbon product HCS-3 derived from HCS-3@mSiO_2 composite pyrolyzed in the absence of surfactant, all pore parameters showed a small difference only. The nitrogen sorption results clearly indicated that confined nanospace pyrolysis of HPS led to the development of additional mesoporosity. In addition, we also measured the porosities of the solid carbon product SCS-1 (from direct pyrolysis of SPS) and SCS-2 (after eliminating the silica shell of SCS-2@SiO_2). As seen in Figure S3, the N_2 sorption isotherm of the SCS-1 was of type I. The hysteresis loop at higher pressure ($P/P_0 = 0.9$-0.997) reflected the inter-samples texture between the particles. Compared with SCS-1, the isotherm of SCS-2 exhibited a step in the relative pressure range of 0.10-0.40 and a hysteresis loop at the relative pressure of 0.42, which were characteristic of some mesopores (Figure S3). These results confirmed that self-activation took place in a confined nanospace by the in situ formed CO_2 and H_2O during pyrolysis in this case but with no hollow core formed.

2,4-dihydroxybenzoic acid molecules contain carboxyl groups which can generate CO_2 during pyrolysis, and thus could be an activating agent responsible for the carbon consumption. To check this possibility, we used a carboxyl-group-free precursor, i.e., phenol instead of dihydroxybenzoic acid to prepare the hollow polymer nanospheres (named HPS*, **Figure 4**a), and consequently silica coated composite (HPS*@SiO_2). The phenolic-based HPS*@SiO_2 was subject to pyrolysis at 800 °C, to obtain carbon sample HCS*-2@SiO_2. As shown in Figure 4b, the hollow cavity were significantly enlarged; approximately 8 times larger than that of the HCS*-1 (Figure 4a inset) derived from HPS* by direct pyrolysis. More intriguingly, after confined pyrolysis, the square core cavity of HPS* were transformed into sphericity with smooth internal surface. It may be attributed to the pressure-tight silica shell, which can trap the in situ generated gases, and facilitate a molecular

small

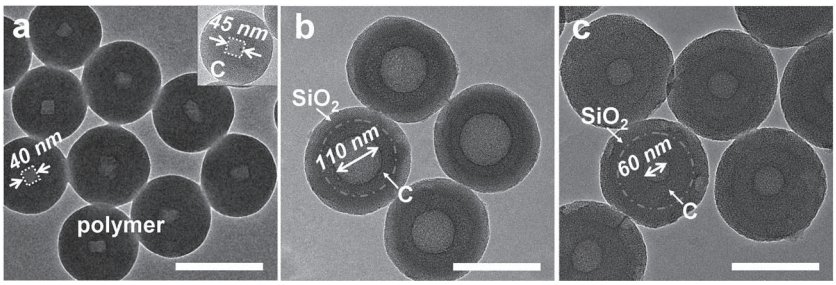

Figure 4. TEM images of a) HPS*, b) HCS*-2@SiO_2, c) HCS*-3@mSiO_2, inset showing the TEM image of HCS*-1, direct pyrolysis of HPS*; scale bars are 200 nm.

self-activation reaction rather than promptly release. In order to open the mesopores to facilitate gas diffusion, composite HPS*@SiO_2 was refluxed by an acidic ethanol solution to remove the CTAB surfactant. The pyrolyzed sample was named as HCS*-3@mSiO_2. As shown in Figure 4c, the hollow core diameter of HCS*-3@mSiO_2 was ca. 60 nm. Though the core sizes of the two carbon products increased, the hollow core expansion was less remarkable than those of HCS-2@SiO_2 and HCS-3@mSiO_2 prepared using carboxyl-containing carbon precursor. This again proved that dihydroxybenzoic acid-based polymer decarboxylated by releasing CO_2 during pyrolysis, which in turn activated the carbon shells.

Coal and char activation by CO_2 and H_2O follows the two main reactions below:[30]

$$CO_2 + C \rightarrow 2CO \quad (1)$$

$$H_2O + C \rightarrow CO + H_2 \quad (2)$$

We estimated the amount of CO_2 and H_2O that could be generated during pyrolysis, by assuming that CO_2 and H_2O are mainly derived from carboxyl and hydroxyl groups (see the Supporting Information for details). Molecules such as dihydroxybenzoic acid, oleic acid, and silanol group could all be considered as potential major contributors. For a specific amount of as-synthesized HPS@SiO_2, we calculated that there is 32 wt% of polymer, and 33 wt% of SiO_2 (Figure S4) residue after pyrolysis at 800 °C in air. Pyrolysis of incomplete condensed silica can release additional H_2O, due to the condensation reaction between adjacent Si-OH groups. To determine the amount of water released from the 33 wt% of SiO_2 from HPS@SiO_2 composite, CTAB-free silica spheres, as a control, were prepared under the same conditions as HPS@mSiO_2 but without using the polymer spheres as seeds. TG-MS analysis confirmed that CTAB had been removed to a great extent. Based on the TG analysis (Figure S4), the estimated weight loss of CTAB-free silica spheres to 800 °C was ~10 wt%, which was due to H_2O release. Finally, 100 mg HPS@SiO_2 would release 0.19 mmol CO_2 and 0.36 mmol H_2O from dihydroxybenzoic acid and oleic acid, and 0.20 mmol H_2O from silanol groups. Following the above Equations (1) and (2), the amount of carbon consumed was estimated to be in the range of 6.60 to 9.00 mg. In general, HPS has typically a 42 wt% carbon yield based on TG analysis. Thus, 100 mg HPS@SiO_2 would in principle generate 13.44 mg carbon. Consequently, the weight loss of carbon owing to CO_2 and H_2O activation was in the range of 49~67 wt%. Assuming carbon consumption from dihydroxybenzoic acid together with oleic acid, or from the silanol group only, it would correspond to 49 wt% and 18 wt%, respectively. However, according to the TEM observation as shown in Figure 1, the actual volume loss of carbon was 50 vol%. On the basis of these results, it seems that the H_2O generated from the outer silica shell mostly diffused outward to the environment, rather into the inner shell, thus not participating in the carbon activation/consumption reaction. The fact that a difference in the nano-architecture design has caused these significant differences in the final structure of the product is worth noting.

In addition, we also calculated the weight of carbon consumption of HPS*@SiO_2 during pyrolysis by assuming that H_2O was mainly derived from hydroxyl groups of phenol and silanol groups. The result was 23.6 wt% and 13.1 wt%, respectively (see the Supporting Information for details). The calculated volume loss of carbon was 23.0 vol%, in accordance with the TEM observation in Figure 4. This also agreed that the H_2O generated from the out silica shell diffused out and did not participate in the carbon activation/consumption. Hence, the theoretical estimations for the two series of samples HPS*@SiO_2 and HPS@SiO_2 agreed well with the experimental observations.

In summary, the hollow core expansion mechanism can be described as follows (**Scheme 1**): during pyrolysis of a hollow polymer nanosphere confined in a silica nanoreactor, an increase in temperature results in the intrinsic thermal shrinkage of silica and carbon (char) materials, leading to an increase in density of the outer shell. The in situ generated

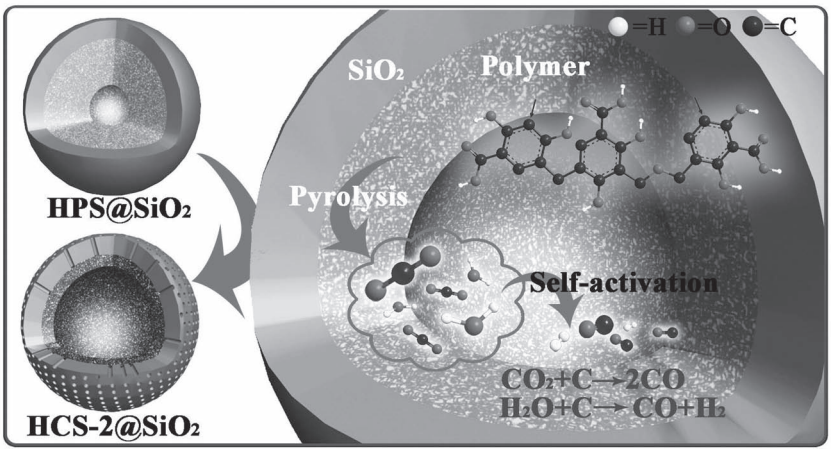

Scheme 1. Schematic illustration for the hollow core expansion of the polymer inside the silica layer nanoreactor.

gases, e.g., CO_2, H_2O, etc, preferentially diffuse into the hollow core open space rather than outside of the core-shell nanostructures. Meanwhile, CO_2 and H_2O partially gasify the in situ formed carbon shells. Until the pressure within the hollow core reaches a critical value, the trapped gases can penetrate the silica and carbon shells to the outer environment. As a consequence, the porosity and the hollow core space increase substantially.

We have demonstrated that a small modification of the shell structure can result in a significant difference in the structure evolution of core-shell composites. The hollow core expansion of core-shell nanostructures as reported here occurs through self-activation in a confined nanospace is unusual. Even more intriguing outcome is the fundamental understanding of the nanoscale details of materials structure development (such as chemical composition, partial decomposition, auto-generated high pressure in the core, enhanced chemical reactivity, and substance release behavior) involves a great deal of confinement effect and interfaces. This discovery may provide a new path to create unique 'nano-atmospheres' with a core-shell nanostructure. The expansion of the hollow structure combined with other inherent properties such as low density, high surface area, thermal insulation and electronic properties etc. adds to the potentials for applications in the fields of controlled drug release, adsorption and catalysis.

Experimental Section

All experimental details are available in the Supporting Information.

Supporting Information

Supporting Information is available from the Wiley Online Library or from the author.

Acknowledgements

The project was supported by NSFC (No. 21073026), National Natural Science Funds for Distinguished Young Scholar (No. 21225312), the Program for New Century Excellent Talents in University of China (NCET-09-0254), and the Scientific Research Foundation for the Returned Overseas Chinese Scholars. We thank Prof. S. Scott at UCSB for the valuable comments on this manuscript.

[1] V. Salgueiriño-Maceira, M. A. Correa-Duarte, *Adv. Mater.* **2007**, *19*, 4131.
[2] R. G. Chaudhuri, S. Paria, *Chem. Rev.* **2012**, *112*, 2373.
[3] S. Wei, Q. Wang, J. Zhu, L. Sun, H. Line, Z. Guo, *Nanoscale* **2011**, *3*, 4474.
[4] S. Ikeda, S. Ishino, T. Harada, N. Okamoto, T. Sakata, H. Mori, S. Kuwabata, T. Torimoto, M. Matsumura, *Angew. Chem. Int. Ed.* **2006**, *45*, 7063.
[5] A. B. Fuertes, M. Sevilla, T. Valdes-Solis, P. Tartaj, *Chem. Mater.* **2007**, *19*, 5418.
[6] A. B. Fuertes, T. Valdes-Solis, M. Sevilla, *J. Phys. Chem. C* **2008**, *112*, 3648.
[7] G. S. Chai, S. B. Yoon, J. H. Kim, J.-S. Yu, *Chem. Commun.* **2004**, 2766.
[8] R. Liu, S. M. Mahurin, R. R. Unocic, J. C. Idrobo, H. Gao, S. J. Pennycook, S. Dai, *Angew. Chem. Int. Ed.* **2011**, *50*, 6799.
[9] X. Fang, Z. Liu, M.-F. Hsieh, M. Chen, P. Liu, C. Chen, N. Zheng, *ACS Nano* **2012**, *6*, 4434.
[10] Z. Lei, Z. Chen, X. S. Zhao, *J. Phys. Chem. C* **2010**, *114*, 19867.
[11] S. Yang, X. Feng, L. Zhi, Q. Cao, J. Maier, K. Müllen, *Adv. Mater.* **2010**, *22*, 838.
[12] L. Guo, L. Zhang, J. Zhang, J. Zhou, Q. He, S. Zeng, X. Cui, J. Shi, *Chem. Commun.* **2009**, 6071.
[13] M. Vallet-Regí, F. Balas, D. Arcos, *Angew. Chem. Int. Ed.* **2007**, *46*, 7548.
[14] Q. Zhang, I. Lee, J. Ge, F. Zaera, Y. Yin, *Adv. Funct. Mater.* **2010**, *20*, 2201.
[15] Y. Deng, Y. Cai, Z. Sun, J. Liu, C. Liu, J. Wei, W. Li, C. Liu, Y. Wang, D. Zhao, *J. Am. Chem. Soc.* **2010**, *132*, 8466.
[16] J. Liu, S. Z. Qiao, J. S. Chen, X. W. Lou, X. Xing, G. Q. Lu, *Chem. Commun.* **2011**, *47*, 12578.
[17] L. Tan, D. Chen, H. Liu, F. Tang, *Adv. Mater.* **2010**, *22*, 4885.
[18] Z. Chen, Z.-M. Cui, F. Niu, L. Jiang, W.-G. Song, *Chem. Commun.* **2010**, *46*, 6524.
[19] J. C. Park, J. U. Bang, J. Lee, C. H. Ko, H. Song, *J. Mater. Chem.* **2010**, *20*, 1239.
[20] J. Lee, J. C. Park, H. Song, *Adv. Mater.* **2008**, *20*, 1523.
[21] X. W. Lou, L. A. Archer, Z. Yang, *Adv. Mater.* **2008**, *20*, 3987.
[22] G.-H. Wang, Q. Sun, R. Zhang, W.-C. Li, X.-Q. Zhang, A.-H. Lu, *Chem. Mater.* **2011**, *23*, 4537.
[23] A.-H. Lu, T. Sun, W.-C. Li, Q. Sun, F. Han, D.-H. Liu, Y. Guo, *Angew. Chem. Int. Ed.* **2011**, *50*, 11765.
[24] S. B. Yoon, J.-Y. Kim, J.-H. Kim, K. R. Yoon, S.-K. Park, S. Yu, *J. Mater. Chem.* **2007**, *17*, 1758.
[25] S. Gai, P. Yang, C. Li, W. Wang, Y. Dai, N. Niu, J. Lin, *Adv. Funct. Mater.* **2010**, *20*, 1166.
[26] J. Kim, H. S. Kim, N. Lee, T. Kim, H. Kim, T. Yu, I. C. Song, W. K. Moon, T. Hyeon, *Angew. Chem. Int. Ed.* **2008**, *47*, 8348.
[27] J. Li, Y. Liu, J. Shi, Z. Wang, L. Hu, X. Yang, C. Wang, *Thermochim. Acta* **2008**, *467*, 20.
[28] M. Dumont, G. Chollon, M. A. Dourges, R. Pailler, X. Bourrat, R. Naslain, J. L. Bruneel, M. Couzi, *Carbon* **2002**, *40*, 1475.
[29] A. Aworn, P. Thiravetyan, W. Nakbanpote, *J. Anal. Appl. Pyrolysis* **2008**, *82*, 279.
[30] J. W. Patrick, *Porosity in Carbons*, Edward Arnold, UK **1995**.

Received: October 27, 2012
Revised: November 21, 2012
Published online: December 27, 2012

